International Journal of Pharmaceutics 390 (2010) 183–190

Contents lists available at ScienceDirect

International Journal of Pharmaceutics

journal homepage: www.elsevier.com/locate/ijpharm

PEG-benzofulvene copolymer hydrogels for antibody delivery

Mariano Licciardi[a], Mario Grassi[b], Mauro Di Stefano[a], Luigi Feruglio[b,c], Germano Giuliani[d], Salvatore Valenti[d], Andrea Cappelli[d], Gaetano Giammona[a,e,*]

[a] Dipartimento di Chimica e Tecnologie Farmaceutiche, via Archirafi 32, 90123 Palermo, Italy
[b] Department of Chemical Engineering DICAMP, Università di Trieste, Piazzale Europa 1, I-34127 Trieste, Italy
[c] Protos Research Institute, via del Follatolo 12, I-34138 Trieste, Italy
[d] Dipartimento Farmaco Chimico Tecnologico and European Research Centre for Drug Discovery and Development, Università degli Studi di Siena, Via A. Moro, 53100 Siena, Italy
[e] IBF-CNR, via Ugo La Malfa, 153, 90143 Palermo, Italy

ARTICLE INFO

Article history:
Received 9 November 2009
Received in revised form 29 January 2010
Accepted 4 February 2010
Available online 11 February 2010

Keywords:
Antibody delivery
Benzofulvene copolymers
Hydrogels
Immunoglobulins

ABSTRACT

Poly[monomethylnona(ethylene glycol) 1-methylene-3-(4-methylphenyl)-1*H*-indene-2-carboxylate] (poly-**1b**) a new polymer based on a PEG-functionalized benzofulvene macromonomer have been investigated as hydrogel-based material for complexation and release of immunoglobulin (IgG) at physiological mimicking conditions.

The polymer ability to complex human IgG has been studied by preparing copolymer/protein complexes obtained by spontaneous protein interactions onto polymer hydrogel aggregates, and the protein release rate has been evaluated at physiological conditions. SEM analysis was used to visualize the copolymer/IgG aggregates and its microstructured deposition. Moreover, rheological studies performed at 37 °C allowed determining hydrogel mechanical properties. On the basis of these information and NMR transverse relaxation measurements, the estimation of hydrogel mesh size distribution was possible.

Finally, biological studies performed with poly-**1b** aqueous dispersions showed no cytotoxic effect on MCF-7 cell line, suggesting potential biocompatibility features for this polymer and making this new polymer a good potential candidate for the production of drug delivery systems.

1. Introduction

The development of novel delivery systems capable of delivering peptide and protein drugs at a controlled rate throughout extended lengths of time is always one of the most important challenge in the field of pharmaceutical research. Implantable drug delivery systems of biocompatible polymers, such as poly(D,L-lactide-co-glycolide) (Bhardwaj and Blanchard, 1997), chitosan and hyaluronic acid (Surini et al., 2003), have been studied for a long time as controlled release systems of pharmaceutically relevant proteins or peptides. Some of these implanted devices were demonstrated to release drugs for an extended period but the necessity of a chirurgical implantation of the device continues to be an obstacle for the compliance of the patients. On the other hand, the delivery of proteins has been recently performed by means of polymeric hydrogels based on physical interactions (Hennink et al., 2004) or by hydrogel (in situ) forming polymeric solutions (Tae et al., 2005) developed to be injected at the implantation site and giving rise to the final hydrogel implant. Undoubtedly, biocompatible synthetic polymeric systems represent promising means for the delivery of many bioactive agents, including peptide and protein drugs. The importance of these systems grew with the advancement in the synthesis of new specialized polymeric materials as well as the understanding of relationship between monomer composition and the physico-chemical properties of the polymer.

Recently, the spontaneous polymerization of benzofulvene derivative **BF1** has been reported to produce a new hydrophobic polymer (poly-**BF1**, Scheme 1) showing a vinyl structure stabilized by aromatic stacking interactions (Cappelli et al., 2003, 2005, 2007).

Poly-**BF1** obtained by spontaneous polymerization showed a very high molecular weight, high solubility in the most common organic solvents, a thermoreversible polymerization/depolymerization, and the tendency to give spontaneously fractal-like macromolecular aggregates (Cappelli et al., 2005). The results obtained in these previous studies demonstrated that most of poly-benzofulvene derivative properties (e.g. formation, molecular weight, structure, thermoreversibility, and aggregation in nanostructured entities) may be modulated by the stereo-electronic characteristics of the substituents present on the indene moiety (Cappelli et al., 2007). Thus, these results stimulated the synthesis of methyl end-capped oligo(ethylene glycol) conjugates

* Corresponding author at: Dipartimento di Chimica e Tecnologie Farmaceutiche, via Archirafi 32, 90123 Palermo, Italy. Tel.: +39 091 6236126; fax: +39 091 6236150.
E-mail address: gaegiamm@unipa.it (G. Giammona).

0378-5173/$ – see front matter © 2010 Elsevier B.V. All rights reserved.
doi:10.1016/j.ijpharm.2010.02.002

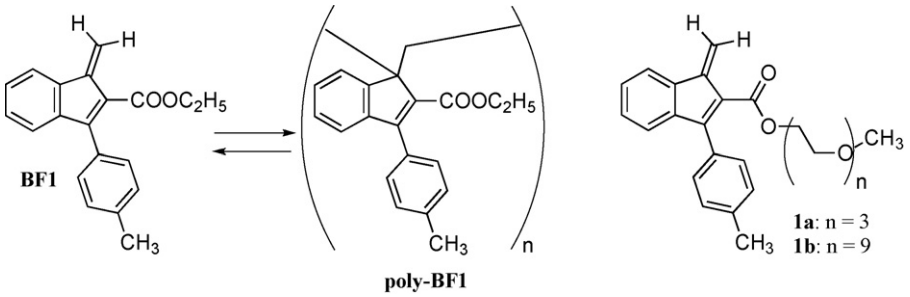

Scheme 1. Structure of benzofulvene derivative **BF1** and MOEG-**BF1** conjugates **1a,b**.

of **BF1** monomer (MOEG-**BF1**, compounds **1a,b** in Scheme 1) by ester linkage of oligo(ethylene glycol) moieties having different ethylene glycol repeating units (n = 3 or 9) in order to evaluate their tendency toward spontaneous polymerization and the properties of the resulting polymers in terms of self-aggregation ability (Cappelli et al., 2009). In particular, poly-MOEG-**BF1** derivative bearing the longer oligo(ethylene glycol) side chain (poly-**1b**) was found to be capable of forming gels stabilized by weak non-covalent interactions (i.e. MOEG chain entanglement and/or π-stacking interactions), and the presence of relatively long MOEG chains allows the interaction with water and the formation of a quite compact physical gel. Owing to the important role played by hydrogels in several fields of the material and life sciences, both the protein interaction and the delivery ability of poly-**1b** hydrogel were investigated in details using human immunoglobulin as model protein drug, and the results of such studies are described herein. For this study, HIgG was chosen as model protein in reason of its well known physical properties, such as spatial dimensions, solubility in function of pH, molecular weight, structure and not for its particular biological properties or activity. Therefore author's goal was to investigate the physical interaction between the model protein and the polymeric matrices and evaluate its influence on protein release profile.

2. Experimental

2.1. Materials and methods

Human immunoglobulin (HIgG) was purchased from Sigma. Ethanol was purchased from Fluka (Switzerland). All the other reagents were of analytical grade. A sample of the previously published poly-**1b** (Cappelli et al., 2009) was used in the complexation/release experiments, rheology, low field NMR studies, and cytotoxicity assays. The weight-average molecular weight (Mw) of the poly-**1b** used in the experiments was 175 kg/mol and the polydispersity index Mw/Mn was 3.0.

Centrifugations were performed using a Centra MP4R IEC centrifuge. UV/vis spectra were recorded with a Shimadzu UV-2401PC spectrophotometer.

2.2. Preparation of HIgG–poly-*1b* complexes

Poly-**1b** (10 mg) was allowed to swell into 2.0 mL of a 1:1 (v/v) water–ethanol mixture at room temperature for 5 days. After this time, ethanol was evaporated under reduced pressure and water removed by freeze drying before protein complexation. Then, 100 μL of the immunoglobulin solution (10 mg/mL) prepared in phosphate buffer solution at pH 6.8 was kept into contact with the lyophilized copolymer and the mixture left to swell 4 days at 4 °C for the impregnation. Impregnation procedure for the preparation of HIgG–poly-**1b** complexes was performed at low temperature (i.e. 4 °C) in order to avoid any degradation phenomena involving protein molecules in aqueous media. In fact, impregnation procedure was efficient after a long period of exposition to the HIgG water solution; and this period was necessary to obtain a complete swelling of the hydrogel. On the other hand, no significant variations of the swelling rate in water were observed by increasing the external temperature to 25 °C in the case of poly-**1b** hydrogels. Then, the excess of protein solution was removed and the swollen copolymer was freeze-dried before protein release studies.

2.3. Immunoglobulin release from HIgG-loaded hydrogels

Freeze-dried poly-**1b**–HIgG complexes prepared as described above, were incubated at 37 °C with PBS solution (3.0 mL, at pH 7.4 or 6.8) into an orbital shaker. At fixed time intervals, 50 μL of supernatant were withdrawn and placed in 1.5 mL centrifuge tube. The volume of the release medium was restored with fresh PBS solution. The samples were then analyzed by HPLC and HIgG release monitored by HPLC during 4 days. HPLC analyses were carried out with an Agilent Liquid Chromatography 1100 Series system (with a 10-μL loop), equipped with a UV Detector 1100 on line with a computerized HP workstation. For release studies, HIgG was analyzed using a SEC Ultrahydrogel 1000 (Waters) column and eluted at a flow rate of 1 mL/min with a mobile phase consisting of a PBS at pH 6.8 (0.05 M KH_2PO_4, 0.12 M Na_2HPO_4, 0.37 M NaCl)/ethanol 95/5, v/v, mixture. HIgG peak was detected at 280 nm.

2.4. Scanning electron microscopy (SEM) analysis

For the morphology studies, poly-**1b**–HIgG samples were dialyzed for 24 h against water and freeze-dried before SEM analysis. Freeze-dried poly-**1b**–HIgG sample were visualized using a scanning electron microscope ESEM Philips XL30. Samples were dusted on a double-sided adhesive tape applied previously on a stainless steel stub. All samples were than sputter-coated with gold prior to microscopy examination.

2.5. Rheology

Hydrogel rheological characterization was performed, at 37 °C, by means of a controlled stress rheometer Haake RheoStress RS150, using, as measuring device, a shagreened plate and plate apparatus (PP35 TI: diameter = 20 mm; gap between plates = 2 mm). The need for this kind of device is due to the necessity of avoiding possible slippage phenomena at the wall. Linear viscoelastic range was determined recurring to stress sweep test consisting in measuring elastic (G') and viscous (G'') moduli variation with increasing deformation (γ) being solicitation frequency f = 1 Hz ($\omega = 2\pi f$ = 6.28 rad/s). Hydrogel mechanical spectrum was determined according to frequency sweep test consisting in measuring elastic (G') and viscous (G'') moduli variation with decreasing pulsation ω at constant deformation stress τ = 20 Pa (well within the linear viscoelastic range).

2.6. Low field NMR

Hydrogel low field NMR characterization was performed by means of a Bruker Minispec mq20 (0.47 T). Transverse relaxation time (T_2) measurement was led according to CPMG (Carr–Purcell–Meiboom–Gill) sequence with 90°–180° pulse separation of 1 ms (number of scans 4; recycle delay 5 s). T_2 distribution was determined by firstly fitting experimental relaxation data by a sum of exponential functions (S) whose number minimized the product $\chi^2 \times N_p$, where χ^2 is data fitting chi-square while N_p is the number of model parameters used (each exponential function considered implies 2 parameters: the pre-exponential factor, A_i, and relaxation time T_{2i}). Then, the continuous relaxation time distribution comes out from the iterative solution of a linear system of equation whose unknowns represents the desired distribution and whose right-hand side column vector represents $S(t_j)$ (t_j is the generic instant time). System matrix coefficient descends from $S(t_j, T_2)$ integration (trapezoid rule) on the continuous relaxation time distribution ($T_{2\min} - T_{2\max}$).

In order to study the effect of swelling procedure on hydrogel structure, two different hydrogel forming techniques were considered. The first consisted in letting the dry polymer (~200 mg) to swell in distilled water (~2 cm^3) at 37 °C up to system transparency (about 10 h). The second one implied dry polymer (~200 mg) swelling at 37 °C in ethanol (~2 cm^3) up to transparency (about 8 h) followed by gel immersion in water (~2 cm^3) at 37 °C for ethanol removal. Every 2 h (for a total of 8 replacements) the swelling medium was completely replaced by pure water (~2 cm^3) at 37 °C in order to ensure the total ethanol removal. Regardless the preparation technique, the freshly prepared hydrogel was put in the rheometer or in the low field NMR measuring device.

2.7. Cytotoxicity assay

Cell viability was assessed by the tetrazolium salt (MTS) assay on MCF-7 cell line (human breast cancer cells obtained from Istituto Zooprofilattico Sperimentale della Lombardia e dell'Emilia Romagna, Italy), using a commercially available kit (Cell Titer 96 Aqueous One Solution Cell Proliferation Assay, Promega). The MTS test is based on the capacity of viable cells to metabolize (via the mitochondrial succinate dehydrogenase) a yellow tetrazolium salt (MTS) in the presence of phenazine methosulfonate (PMS) acting as an electron coupling agent. The reaction yields a purple formazan that is directly soluble in tissue culture medium and the absorbance at 490 nm is measured, which is proportional to the number of living cells.

MCF-7 cells were maintained in minimum essential medium Eagle (MEM) containing 10% foetal bovine serum, and 1% of penicillin/streptomycin (100 U/mL penicillin and 100 μg/mL streptomycin), at 37 °C in 5% CO_2 humidified atmosphere. Cells were seeded at 5×10^4 cell/well in 200 μL of complete medium in a 96-wells microtiter plate and allowed to adhere for 72 h.

After 72 h, cells were treated with poly-**1b** solutions prepared as it follows: polymer samples were swollen in ethanol at room temperature for 1 week under continuous shaking. After this time, the ethanol excess was removed from the micro-gel aggregates and replaced with sterile MEM. The aqueous dispersion was than stirred for further 3 days. UV spectroscopy analysis evidenced the presence of the polymer in the aqueous solution, at a concentration of about 1000 μM (in monomer base unit, as determined by UV detection at 290 nm). Subsequently, 10, 20 and 40 μL of this polymer dispersion were added to the cell preparations in fresh medium (giving a final volume of 200 μL and a final monomer concentration of 50, 100 and 200 μM, respectively) and incubated for 24 or 72 h. After incubation, 20 μL of MTS reagent solution (0.5 mg/mL) were added to each well and plates were incubate for additional 2 h at 37 °C. The absorbance at 490 nm was measured using a Microplate reader (Multiskan Ex, Thermo Labsystems, Finlandia). Relative cell viability (percentage) was expressed as (Abs_{490} treated cells/Abs_{490} control cells)/100, as an average of ten values. Cells incubated with fresh medium were used as negative control (data not reported) and in presence of linear polyethylene imine (PEI, 22 kDa), at 100 μM monomer amine units, as positive control.

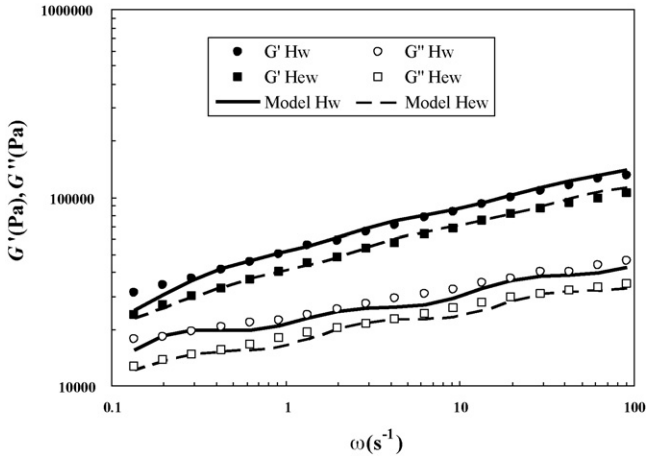

Fig. 1. Hydrogels mechanical spectra. Filled and open circles indicate, respectively, the elastic (G'_{Hw}) and the viscous (G''_{Hw}) modulus referring to the hydrogel swollen in water (H_w). Filled and open squares indicate, respectively, the elastic (G'_{Hew}) and the viscous (G''_{Hew}) modulus referring to the hydrogel swollen in ethanol and then in water (H_{ew}). Solid and dashed lines indicate generalized Maxwell model best fitting referring, respectively, to H_w and H_{ew} hydrogels. ω is pulsation (=$2\pi f$, f= solicitation frequency).

2.8. Statistical analysis

A one-way analysis of variance (ANOVA) was used to evaluate group comparison. If the group by each time interaction was significantly different ($P < 0.05$), differences between groups were compared within a posteriori Bonferroni t-test. All the values are reported as the average ± standard deviation. The standard deviation values (±S.D.) were calculated on the basis of three experiments conducted in multiples of ten.

3. Results and discussion

3.1. Rheology—low field NMR

Stress sweep tests revealed that for the hydrogel directly swollen in water (H_w) the linear viscoelastic range spans up to a critical deformation/stress equal to 1% and 480 Pa, respectively. On the contrary, for the hydrogel swollen in ethanol and then in water (H_{ew}), the linear viscoelastic range spans up to a critical deformation/stress equal to 0.5% and 320 Pa, respectively. Accordingly, in order to be in the linear viscoelastic regime, frequency sweep tests were performed, for both hydrogels, at a constant stress equal to 20 Pa. Fig. 1 shows that for both hydrogels, mechanical spectra, represented by the elastic (G') and viscous (G'') modulus trend versus pulsation ω (=$2\pi f$, f= solicitation frequency), are similar although H_w is characterized by higher values of G' and G''. As G' is always bigger than G'', the elastic properties are always predominant on the viscous ones for both hydrogels. Fig. 1 and Table 1 also show that G' and G'' trends referring to the H_w hydrogel can be satisfactory fitted by means of the generalized Maxwell model constituted by 5 elements (mechanical devices each one composed by a spring and a dashpot in series) put in parallel whose relaxation times λ_i are scaled in reason of ten and whose last (nth) element is repre-

Table 1
Generalized Maxwell model fitting parameters referring to the hydrogel swollen in water (H_w) and to the hydrogel swollen in ethanol and then in water (H_{ew}). λ_1 is the first Maxwell element relaxation time, while $G_1, G_2, \ldots, G_\infty$ indicate springs constants. Best fitting parameters are reported as mean ± standard deviation, while F is the F statistic.

	H_w $F(6,36,0.99) < 550$	H_{ew} $F(5,36,0.99) < 181$
λ_1 (s)	$(4.3 \pm 0.6) \times 10^{-3}$	$(3.1 \pm 0.4) \times 10^{-3}$
G_∞ (Pa)	17,240 ± 2246	4633 ± 1526
G_1 (Pa)	86,429 ± 5811	70,247 ± 3323
G_2 (Pa)	50,254 ± 4735	41,703 ± 2274
G_3 (Pa)	32,838 ± 2809	30,202 ± 1524
G_4 (Pa)	30,328 ± 2461	19,509 ± 1213
G_5 (Pa)	–	15,883 ± 1550

sented by a pure elastic spring of constant G_∞ (Lapasin and Pricl, 1995):

$$G' = G_\infty + \sum_{i=1}^{n-1} G_i \frac{(\lambda_i \omega)^2}{1 + (\lambda_i \omega)_i^2} \quad (1)$$

$$G'' = \sum_{i=1}^{n} G_i \frac{\omega \lambda_i}{1 + (\lambda_i \omega)^2}; \quad (2)$$

where G_i represent springs elastic constants.

On the contrary, six Maxell elements are needed to describe the mechanical spectrum of the H_{ew} hydrogel (see Fig. 1 and Table 1).

Assuming that hydrogel shear modulus G is the sum of the elastic contributes (G_i) of each Maxwell element (Pasut et al., 2008), hydrogel crosslink density ρ_x can be evaluated by (Flory, 1953):

$$\rho_x = \frac{G \nu_p^{2/3}}{RT} \quad (3)$$

where R is universal gas constant, T is absolute temperature and ν_p is polymer volume fraction in the gel. For the H_w gel, Eq. (3) yields $\rho_x = (2.4 \pm 0.4) \times 10^{-5}$ mol/cm^3 being $\nu_p = (0.15 \pm 0.01)$ and $G = (217042 \pm 8671)$ Pa. For the H_{ew} gel, instead, Eq. (3) yields $\rho_x = (1.9 \pm 0.2) \times 10^{-5}$ mol/cm^3 being $\nu_p = (0.14 \pm 0.006)$ and $G = (182180 \pm 4974)$ Pa. Interestingly, on the basis of ρ_x knowledge and the "equivalent network theory" (Schurz, 1991), it is possible estimating the average mesh size of the polymeric network. As a detailed description is impossible, this theory replaces polymeric network by an idealized network made by a collection of blobs whose diameter coincides with the average network mesh size φ according to the following relation:

$$\varphi = \sqrt[3]{\frac{6}{\pi N_{av} \rho_x}} \quad (4)$$

where N_{av} is the Avogadro number. Accordingly, we have $\varphi = (5.1 \pm 0.3)$ nm and $\varphi = (5.5 \pm 0.2)$ nm for the H_w and H_{ew} hydrogels, respectively. Thus, we can conclude that the two hydrogels are, substantially, equal for what concerns rheological macro-properties and structural micro-properties.

In order to obtain deeper information about hydrogel structure, a low field NMR characterization has been undertaken as this technique can provide useful information via the determination of hydrogen atoms status. Indeed, this approach can, in principle, discriminate among hydrogen atoms belonging to the polymeric chains, to the water entrapped inside polymeric meshes, to the water trapped inside hydrogel channels and to water external to the hydrogel structure. The working principle of this approach relies on the reduction of the transverse relaxation time (T_2) of hydrogen atoms characterized by reduced mobility as it happens for hydrogen atoms belonging to polymeric chains or to the water confined

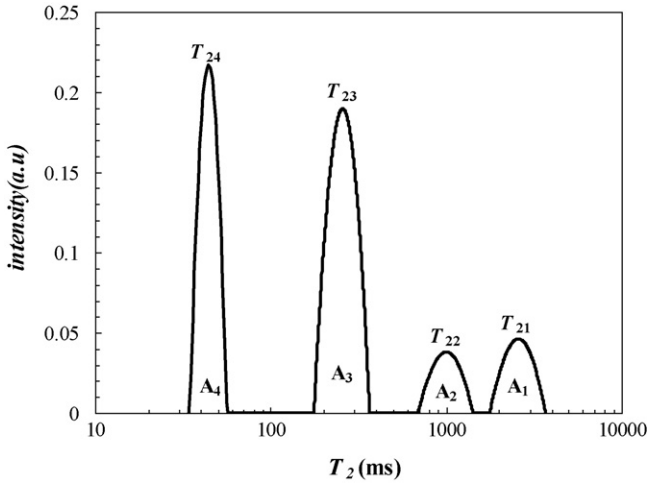

Fig. 2. Hydrogel H_w transverse relaxation time T_2 distribution. Four peaks (1, 2, 3 and 4) characterize T_2 distribution. A_1, A_2, A_3 and A_4 indicate peak area while T_{21}, T_{22}, T_{23} and T_{24} indicate the respective transverse relaxation time occurring at peak maximum. Similar T_2 distribution can be obtained for the H_{ew} hydrogel.

inside polymeric meshes (Brownstein and Tarr, 1979). Fig. 2, showing hydrogel H_w T_2 distribution, evidences the existence of four peaks witnessing the existence of four hydrogen atom conditions in the hydrogel. Remembering that we are dealing with a not perfectly homogeneous system (it is a sort of highly concentrated suspension of homogeneous gel particles), the existence of the four peaks can be explained as follows. On the basis of high transverse relaxation time ($T_{21} = 2571$ ms; $A_1 = 56$), the first peak on the right represents the amount of hydrogen atoms belonging to water that is out of the ensemble of gel particles. Indeed, gel presence determines only a minor reduction on transverse relaxation (pure water hydrogen atoms transverse relaxation time at 37 °C is around 3100 ms). The second peak from the right ($T_{22} = 1000$ ms, $A_2 = 17$) corresponds to hydrogen atoms belonging to the water entrapped among gel particles (gel channels). On the contrary the third peak ($T_{23} = 256$ ms, $A_3 = 23$) corresponds to hydrogen atoms belonging to the water inside gel particles polymeric network. Finally, the fourth peak ($T_{24} = 44$ ms, $A_4 = 3$), in virtue of low transverse relaxation time, corresponds to polymer hydrogen atoms. Absolutely similar results can be obtained for the H_{ew} hydrogel.

The correctness of this interpretation was discussed elsewhere (Cappelli et al., 2009). Accordingly, it is now possible extending our knowledge on hydrogel network structure remembering that the shape of peak 3 is strictly correlated with polymeric mesh size distribution (Halperin et al., 1989). Indeed, it is well known (Brownstein and Tarr, 1979) that the T_2 of hydrogen atoms belonging to the water trapped inside polymeric mesh (also called polymer nanopores) is proportional to nanopore diameter ξ via a constant (k) depending only on pore geometry (spherical, cylindrical, and so on) and inner surface properties. Thus, the information coming from rheology and low field NMR can be profitably combined to yield nanopores size distribution. k evaluation is based on the relation existing between peak 3 average transverse relaxation time $\overline{T}_{23}$ and average diameter φ:

$$\overline{T}_{23} = \frac{\int_{T_{23\min}}^{T_{23\max}} I_3(T_2) \times T_2 \times dT_2}{\int_{T_{23\min}}^{T_{23\max}} I_3(T_2) \times dT_2} \overbrace{=}^{T_2 = k\xi} \frac{k^2 \int_{k\xi_{2\min}}^{k\xi_{23\max}} I_3(\xi) \times \xi \times d\xi}{k \int_{k\xi_{23\min}}^{k_2\xi_{23\max}} I_3(\xi) \times d\xi}$$

$$= k\varphi \overbrace{=}^{\text{Eq. (4)}} k \sqrt[3]{\frac{6}{\pi N_{av} \rho_x}} \quad (5)$$

where I_3 is peak 3 local intensity, $T_{23\max}$ (or $\xi_{23\max}$) and $T_{23\min}$ (or $\xi_{23\min}$) indicate peak 3 extension in terms of transverse relaxation

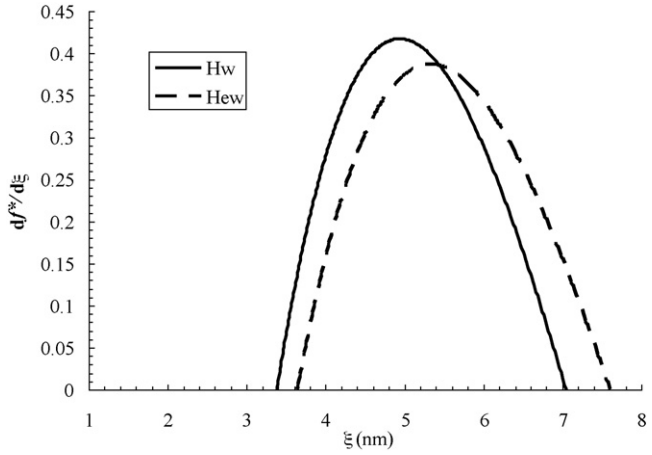

Fig. 3. Hydrogels H_w and H_{ew} mesh size distribution. On the basis of the information coming from the rheological and low field NMR analysis, it is possible getting the differential mesh size distribution normalized versus the total pores volume ($df^*/d\xi$). ξ is mesh size.

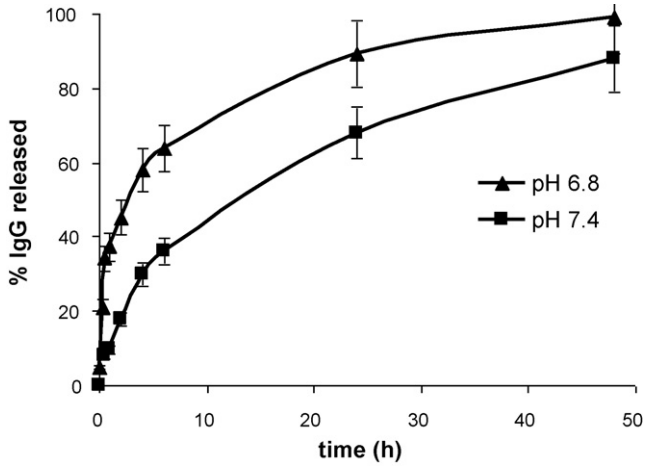

Fig. 4. Plot of the released percentage amount of protein versus time.

time (or pores diameter). Thus, k can be evaluated as

$$k = \frac{\overline{T}_{23}}{\sqrt[3]{6/\pi N_{av}\rho_x}} \quad (6)$$

For the H_w and H_{ew} hydrogels, k is equal to 52 (ms/nm) and 48 (ms/nm), respectively. Once T_2 is converted into pore diameter, it is possible determining the differential pore size distribution normalized versus the total pores volume ($df^*/d\xi$) as shown in Fig. 3 for both hydrogels.

It is evident that both hydrogels do not significantly differ for what concerns mesh size distribution. In addition, these systems are characterized by meshes spanning from about 3.5 nm up to 7.5 nm. Accordingly, only small molecules can be hosted inside their polymeric networks.

3.2. Release studies

Poly-**1b** is a synthetic polymer showing π-stacking features and aggregate formation ability, which appears as a colourless elastic sticky solid (Cappelli et al., 2009). It shows affinity and swelling ability with a number of organic solvents (e.g. chloroform, THF, DMF, DMA, DMSO, ethanol, and methanol) and with water generating transparent gel aggregates characterized by high compactness (Cappelli et al., 2009). Thus, when poly-**1b** is swollen in ethanol at room temperature for 1 week and the ethanol excess is removed from the gel aggregates and replaced with water no evident changes are observed in gel appearance (Cappelli et al., 2009). These results suggested that the addition of a protein solution instead of pure water may generate the migration of protein molecules from the bulk solution to the gel matrix depth with the consecutive physical interaction of protein with poly-**1b**; actually, the nature and entity of the interaction should be dependent by the protein type. Using human IgG as an antibody protein model we observed a high efficiency of impregnation of poly-**1b** hydrogels, as demonstrated by HIgG release studies in aqueous media.

Two types of release media were used for evaluating the HIgG release rate from poly-**1b** hydrogel: one being PBS at pH 6.8, mimicking intestinal fluids pH conditions; and the other being PBS at pH 7.4, mimicking interstitial fluids and plasma pH. Even if phosphate buffer only partially represent intestinal fluids (simulated intestinal fluid (SIF) includes the presence of bile salts as well), in this case the presence of bile salts may cause protein degradation and make impossible its detection. Actually, release studies here reported provide a experimental proof of the ability of the hydrogel to release the model protein HIgG as a function of pH, without any influence attributed to the modification of protein morphology or structure. In the two different pH condition we observed a biphasic and prolonged HIgG release profile (see Fig. 4): a relatively low first burst release, probably due to solvation of HIgG adsorbed onto hydrogel surface and promptly released, and a second slower release phase mainly controlled by diffusion of the large immunoglobulin through hydrogel channels and hydrogel swelling rate in the aqueous medium (Kim et al., 2003; Hennink et al., 1996). As shown in Fig. 4, the comparison of protein release profile at the two different pH values suggests a slower HIgG release rate at pH 7.4 than at pH 6.8. In the latter case HIgG release from poly-**1b** hydrogel resulted complete after 48 h of incubation and corresponded to the total protein amount loaded into the hydrogel, i.e. 5%, w/w (70% of the protein amount present into the protein solution used for hydrogel impregnation. This protein amount was determined by the difference between the protein amount before hydrogel impregnation and that after hydrogel impregnation; the latter was obtained by freeze drying the surnatant after the protein loading into the hydrogel). As hydrogel swelling does not depend on temperature and pH (at least in the temperature and pH range here considered), the different release kinetics observed at pH = 6.8 and 7.4 depend on the different HIgG solubility (~68 mg/mL at pH 6.8 and ~50 mg/mL at pH 7.4) experimentally determined. Moreover, HPLC analysis of HIgG used to evaluate protein release give undoubtedly the warranty of protein integrity and activity.

3.3. Microscopy analysis

SEM studies revealed the presence of protein aggregates on the lyophilized hydrogel surface (see Fig. 5). The protein molecules dislocated in the periphery, in contact with the bulk aqueous medium rapidly dissolve, thus justifying the initial burst protein release shown in the release profile.

However, the SEM images revealed the presence of immunoglobulin crystals (white cylinders in Fig. 6) internally to the gel fractures probably produced by cryogenic freezing, i.e. liquid nitrogen immersion of the hydrogels before lyophilization.

On the basis of the HIgG big dimensions (height = 14.5 nm, width = 8.5 nm, thickness = 40 nm) (Lee et al., 2002) and the evaluation of mesh size distribution previously studied (3.5 nm < ξ < 7.5 nm), we can conclude that the presence of HIgG inside the polymeric network is not very probable. On the contrary, it is reasonable that it mainly relies on the surface of gel channels whose presence, in the swollen state, has been proved by the low field NMR analysis (see Fig. 2, peak A_2). Thus, release

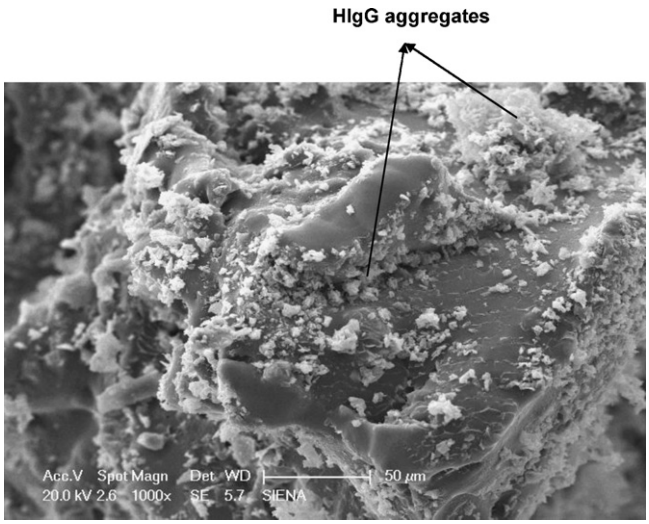

Fig. 5. SEM image of HIgG-loaded poly-**1b** lyophilized sample at 1000× magnification.

kinetics should be mainly ruled by the dissolution, in the incoming swelling agent (water), of HIgG coating hydrogel channels. This hypothesis could explain the initial burst release due to the fast dissolution of HIgG coating in the more external part of hydrogel channels that are immediately wet by the dissolution medium (water). The second, slower release phase should be controlled by water penetration inside matrix channels and the following HIgG dissolution and diffusion in the water filled hydrogel channels. The release kinetics of this second step should be also controlled by the interaction taking place between HIgG and channel surface.

3.4. Interaction of HIgG with the hydrogel surface

The protein-polymer interaction between HIgG and the hydrogel surface can be evaluated by estimating the partition coefficient k_p expressing the ratio between the HIgG concentration in the gel phase and in the release environment at equilibrium. Let's suppose to put a known amount of the dry, HIgG free, polymeric matrix in an aqueous HIgG solution of known volume (V_{s0}) and concentration (C_{s0}). After a very long time, the equilibrium between the gel phase and the external solution will be met. At this time, the following mass balance must hold:

$$C_{g\infty}V_{g\infty} + C_{s\infty}V_{s\infty} = C_{s0}V_{s0} \tag{7}$$

where $C_{g\infty}$ and $C_{s\infty}$ are, respectively, HIgG concentration in the gel phase and in the external solution, while $V_{g\infty}$ and $V_{s\infty}$ represent, respectively, gel and solution volumes. Eq. (7) simply states that the sum of the HIgG amount in the gel phase ($C_{g\infty}$ $V_{g\infty}$) and in the solution ($C_{s\infty}$ $V_{s\infty}$) must be equal to the HIgG amount originally present in the solution (C_{s0} V_{s0}). As we know that 70% of the original HIgG amount present in the solution went in the gel phase, we have:

$$C_{g\infty}V_{g\infty} = 0.7C_{s0}V_{s0} \Rightarrow C_{g\infty} = 0.7\frac{C_{s0}V_{s0}}{V_{g\infty}} \tag{8}$$

$$C_{s\infty}V_{s\infty} = 0.3C_{s0}V_{s0} \Rightarrow C_{s\infty} = 0.3\frac{C_{s0}V_{s0}}{V_{s\infty}} \tag{9}$$

Thus:

$$k_p = \frac{C_{g\infty}}{C_{s\infty}} = 2.33\frac{V_{s\infty}}{V_{g\infty}} \tag{10}$$

As $V_{s\infty}$ and $V_{g\infty}$ can be expressed by

$$V_{s\infty} = V_{s0} - V_p\frac{(1-\nu_p)}{\nu_p} \qquad V_{g\infty} = V_p + V_p\frac{(1-\nu_p)}{\nu_p} \tag{11}$$

where V_p (=7.7×10^{-3} cm^3) is polymer volume, ν_p (=0.14) is polymer volume fraction at equilibrium and V_{s0} (=0.1 cm^3) is initial solution volume, the partition coefficient k_p results to be approximately 2.27. This proves that HIgG shows a higher affinity for the gel environment with respect to the release environment.

3.5. Biological properties

For polymers used in drug delivery, the lack of toxicity is a fundamental property. For this reason, the biological properties of

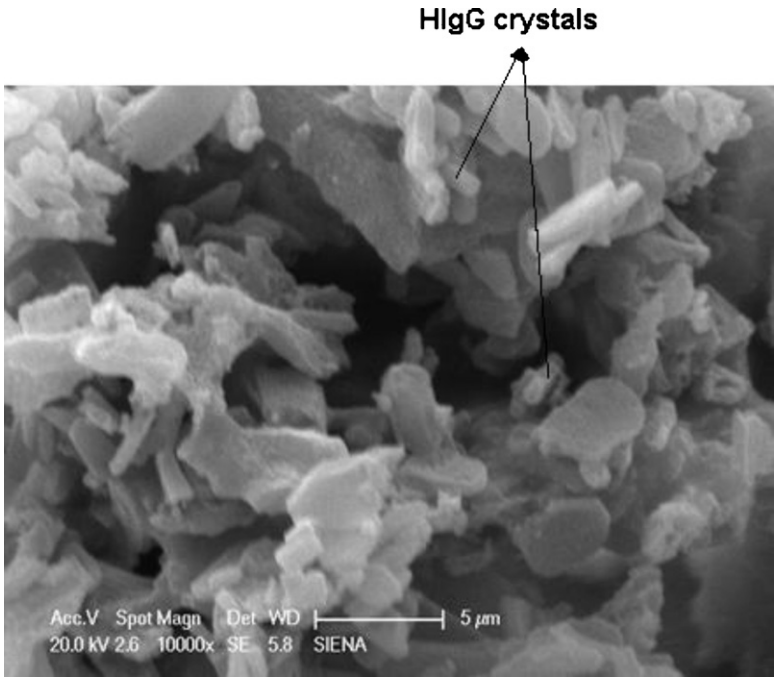

Fig. 6. SEM image of HIgG-loaded poly-**1b** lyophilized sample at 10,000× magnification.

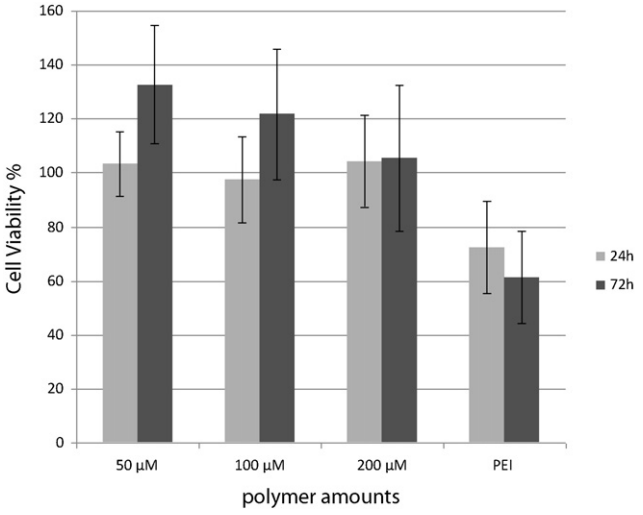

Fig. 7. cell viability evaluated by MTS tests in human cancer cell line (MCF-7) incubated at 37 °C in the presence of the polymer dispersions (50, 100 and 200 μM in monomer units) for either 24 or 72 h; as positive control PEI-treated cells (100 μM in monomer units) were included. Data are shown as mean ± S.D., $n = 10$.

poly-**1b** were evaluated again using dispersions containing crescent polymer concentrations (corresponding to 50, 100 and 200 μM in monomer base unit) and a cellular line different from those used previously (Cappelli et al., 2009). Indeed, the potential toxicity of poly-**1b** was tested in vitro on human cancer cell line MCF-7. The epithelial breast cancer derived MCF-7 cell line is one of the most frequently used model systems in studies concerning treatment of breast cancer. Many groups have reported that the proliferative response of MCF-7 cells is particularly sensible to the medium composition (Van der Burg et al., 1988; Hamelers et al., 2003). In general, as it can be seen in Fig. 7, poly-**1b** resulted not toxic at the concentrations investigated in the present work. In particular, cell viability observed after 72 h of incubation with poly-**1b** seems to exceed 100%, at the lower polymer concentrations tested. Cell viability was also tested in presence of linear PEI (at 100 μM in monomer base unit) as a positive control. In this case the expected toxic effects of PEI (Klemm et al., 1998; Cavallaro et al., 2006) on MCF-7 cells, confirmed the absence of antiproliferative effect of poly-**1b**.

Thus, the preliminary results obtained suggest that poly-**1b** hydrogel could find application as component of gastro-resistant oral formulation for sustained release of proteins. On another hand, being the hydrogel used in this study based on physical interaction (oligo-PEG chain entanglement and π-stacking interactions of benzofulvene moieties) rather than covalent linkages, the gel may be converted reversibly to sol by disrupting the associations above mentioned to create injectable depots. Application of this capability depends upon the possibility to achieve the sol state in a biocompatible liquid, and recovering the gel state spontaneously in situ, retaining the native structure of the therapeutic protein and release it with time. Many authors reported the possibility to dissolving the gel forming polymer in a solvent (or solvent/water mixture) with a bio-tolerable and water miscible organic solvent, such as NMP or DMSO, obtaining a sufficiently low viscosity which permit injection by means of a syringe (Joshi et al., 1998; Pitarresi et al., 2008). Consequently, the contact with the aqueous physiological environment induces the restoration of the gel state and the formation of a depot from which protein can be slowly released in situ. These considerations may be the goal for a future investigation on poly-**1b** biomedical application.

4. Conclusions

The hydrogel obtained by physical interactions of poly[monomethylnona(ethylene glycol) 1-methylene-3-(4-methylphenyl)-1*H*-indene-2-carboxylate] (poly-**1b**), a new polymer based on a PEG-functionalized benzofulvene moiety, has been investigated in order to evaluate its properties as a material for complexation and release of immunoglobulin (IgG) in physiological mimicking conditions.

Poly-**1b** hydrogel was loaded with HIgG by imbibition of dry poly-**1b** matrix with the protein solution and was found to be able to release the loaded protein in physiological mimicking media. The protein release rate evaluated at pH 6.8 and 7.4 revealed a pH-dependence profile and the hydrogel ability to release HIgG in the intact form for a period not inferior to 48 h. In the light of its big dimensions, the loaded HIgG should not be present inside the hydrogel network, but it should be mainly found on the surface of the channels pervading poly-**1b** matrix. Accordingly, release kinetics should not be controlled by diffusion. On the contrary, it should depend on HIgG dissolution rate (depending on pH), water uptake and the high HIgG interaction with poly-**1b** surface.

Finally, biological studies performed with poly-**1b** water solutions showed no cytotoxicity on human breast cancer cells line confirming potential biocompatibility features for this polymer. In conclusion, poly-**1b** can be considered a promising polymer for the preparation of hydrogels potentially useful in a range of biological and biotechnological applications, in particular for drug delivery, as component of gastro-resistant oral formulation for sustained release of proteins or in situ gel forming from which protein can be slowly released upon injection of the gel depot in situ.

Acknowledgment

Authors thank MIUR for funding.

References

Bhardwaj, R., Blanchard, J., 1997. In vitro implants evaluation of poly(D,L-lactide-co-glycolide) polymer-based containing the α-melanocyte stimulating hormone analog, Melanotan-I. J. Control. Release 45, 49–55.
Brownstein, K.R., Tarr, C.E., 1979. Importance of classical diffusion in NMR studies of water in biological cells. Phys. Rev. A 19, 2446–2452.
Cappelli, A., Anzini, M., Vomero, S., Donati, A., Zetta, L., Mendichi, R., et al., 2005. New π-stacked benzofulvene polymer showing thermoreversible polymerization: studies in macromolecular and aggregate structures and polymerization mechanism. J. Polym. Sci. A: Polym. Chem. 43, 3289–3304.
Cappelli, A., Galeazzi, S., Giuliani, G., Anzini, M., Donati, A., Zetta, L., et al., 2007. Structural manipulation of benzofulvene derivatives showing spontaneous thermoreversible polymerization. Role of the substituents in the modulation of polymer properties. Macromolecules 40, 3005–3014.
Cappelli, A., Galeazzi, S., Giuliani, G., Anzini, M., Grassi, M., Lapasin, R., et al., 2009. Synthesis and spontaneous polymerization of oligo(ethylene glycol)-conjugated benzofulvene macromonomers. A polymer brush forming a physical hydrogel. Macromolecules 42, 2368–2378.
Cappelli, A., Pericot Mohr, G., Anzini, M., Vomero, S., Donati, A., Casolaro, M., et al., 2003. Synthesis and characterization of a new benzofulvene polymer showing a thermoreversible polymerization behaviour. J. Org. Chem. 68, 9473–9476.
Cavallaro, G., Campisi, M., Licciardi, M., Ogris, M., Giammona, G., 2006. Reversibly stable thiopolyplexes for intracellular delivery of genes. J. Control. Release 115, 322–334.
Flory, P.J., 1953. Principles of Polymer Chemistry. Cornell University, Ithaca, NY.
Halperin, W.P., D'Orazio, F., Bhattacharja, S., Tarczon, T.C., 1989. Magnetic Resonance Relaxation Analysis of Porous Media. John Wiley and Sons, New York.
Hamelers, H.L.I., van Schaik, R.F.M.A., Sussenbach, J.S., Steenbergh, P.H., 2003. 17β-Estradiol responsiveness of MCF-7 laboratory strains is dependent on an autocrine signal activating the IGF type I receptor. Cancer Cell Int. 3, 10.
Hennink, W.E., De Jong, S.J., Bos, G.W., Veldhuis, T.F.J., van Nostrum, C.F., 2004. Biodegradable dextran hydrogels crosslinked by stereocomplex forming for the controlled release of pharmaceutical proteins. Int. J. Pharmacol. 227, 99–104.
Hennink, W.E., Talsma, H., Borchert, J.C.H., De Smedt, S.C., Demeester, J., 1996. Controlled release of proteins from dextran hydrogel. J. Control. Release 39, 47–55.

Joshi, R., Arora, V., Desjardines, J.P., Robinson, D., Himmelstein, K.J., Iversen, P., 1998. In vivo properties of an in situ forming gel for parenteral delivery of macromolecular drugs. Pharmacol. Res. 15, 1189–1195.

Kim, B., La Flamme, K., Peppas, N.A., 2003. Dynamic swelling behaviour of pH-sensitive anionic hydrogels used for protein delivery. J Appl. Polym. Sci. 89, 1606–1613.

Klemm, A.R., Young, D., Lloyd, J.B., 1998. Effects of polyethyleneimine on endocytosis and lysosome stability. Biochem. Pharmacol. 56, 41–46.

Lapasin, R., Pricl, S., 1995. Rheology of Industrial Polysaccharides, Theory and Applications. Chapman & Hall, London.

Lee, K.B., Park, S.J., Mirkin, C.A., Smith, J.C., Mrksich, M., 2002. Protein nanoarrays generated by dip-pen nanolithography. Science 295, 1702–1705.

Pasut, E., Toffanin, R., Voinovich, D., Pedersini, C., Murano, E., Grassi, M., 2008. Mechanical and diffusive properties of homogeneous alginate gels in form of particles and cylinders. J. Biomed. Mater. Res. A 87A, 819–824.

Pitarresi, G., Palumbo, F.S., Albanese, A., Licciardi, M., Calascibetta, F., Giammona, G., 2008. In situ gel forming graft copolymers of a polyaspartamide and polylactic acid: preparation and characterization. Eur. Polym. J. 44, 3764–3775.

Schurz, J., 1991. Rheology of polymer solution of the network type. Prog. Polym. Sci. 16, 1–53.

Surini, S., Akiyama, H., Morishit, M., Nagai, T., Takayama, K., 2003. Release phenomena of insulin from an implantable device composed of a polyion complex of chitosan and sodium hyaluronate. J. Control. Release 90, 291– 301.

Tae, G., Kornfield, J.A., Hubbell, J.A., 2005. Sustained release of human growth hormone from in situ forming hydrogels using self-assembly of fluoroalkyl-ended poly(ethylene glycol). Biomaterials 26, 5259–5266.

Van der Burg, B., Rutteman, G.R., Blankenstein, M.A., De Laat, S.W., Van Zoelen, E.J.J., 1988. Mitogenic stimulation of human breast cancer cells in a growth factor-defined medium: synergistic action of insulin and estrogen. J. Cell Physiol. 134, 101–108.